Fast Green's Function Method for Ultrafast Electron-Boson Dynamics

Daniel Karlsson,[1] Robert van Leeuwen,[1] Yaroslav Pavlyukh,[2,3] Enrico Perfetto,[3,4] and Gianluca Stefanucci[3,4]
[1]Department of Physics, Nanoscience Center, University of Jyväskylä, P.O. Box 35, FI-40014 Jyväskylä, Finland
[2]Institut für Physik, Martin-Luther-Universität Halle-Wittenberg, 06120 Halle, Germany
[3]Dipartimento di Fisica, Università di Roma Tor Vergata, Via della Ricerca Scientifica 1, 00133 Rome, Italy
[4]INFN, Sezione di Roma Tor Vergata, Via della Ricerca Scientifica 1, 00133 Rome, Italy

(Received 26 June 2020; revised 29 March 2021; accepted 20 May 2021; published 15 July 2021)

The interaction of electrons with quantized phonons and photons underlies the ultrafast dynamics of systems ranging from molecules to solids, and it gives rise to a plethora of physical phenomena experimentally accessible using time-resolved techniques. Green's function methods offer an invaluable interpretation tool since scattering mechanisms of growing complexity can be selectively incorporated in the theory. Currently, however, real-time Green's function simulations are either prohibitively expensive due to the *cubic* scaling with the propagation time or do neglect the feedback of electrons on the bosons, thus violating energy conservation. We put forward a computationally efficient Green's function scheme which overcomes both limitations. The numerical effort scales *linearly* with the propagation time while the simultaneous dressing of electrons and bosons guarantees the fulfillment of all fundamental conservation laws. We present a real-time study of the phonon-driven relaxation dynamics in an optically excited narrow band-gap insulator, highlighting the nonthermal behavior of the phononic degrees of freedom. Our formulation paves the way to first-principles simulations of electron-boson systems with unprecedented long propagation times.

DOI: 10.1103/PhysRevLett.127.036402

The time-dependent behavior of systems with strongly interacting electrons and bosons (EBs) is attracting increasing attention [1]. Plasmon-polariton physics in semiconductors [2–4], light-enhanced electron-phonon (*e*-ph) driven superconductivity [5–8], electron-magnon hybridization-induced zero-bias anomalies in quantum transport [9,10], manipulation of the thermoelectricity with cavity photons [11], and the new field of light-driven chemistry [12] which aims at modifying chemical reaction landscapes through strong coupling of matter to quantized photons [13], is a nonexhaustive list of possible applications. A fast and first-principles tool to deal with the quantized nature of bosons is thus an essential requirement for future material-specific predictions. Furthermore, such a tool may also open the way to more sophisticated approximations of purely electronic systems, as the screened Coulomb repulsion can be viewed as a bosonic propagator.

A full-fledged many-body method for realistic time-dependent EB systems is challenging, however, as the quantum nature of both species has to be taken into account on the same footing [14,15]. Methods such as the direct solution of the Schrödinger equation for the electron-boson wave function or quantum Monte Carlo methods [16], scale exponentially with system size and/or time [17], while other methods, such as the time-dependent matrix renormalization group [18], are limited to model systems with a relatively small number of basis functions. A computationally low-cost method is the extension of time-dependent density-functional theory (DFT) to quantized bosons [19–21], with a linear scaling in time and a power-law scaling with system size. Nevertheless, like standard DFT, this extension suffers from a lack of systematicity in generating approximate functionals, as well as issues in including nonadiabatic effects.

EB interactions can instead be treated systematically through diagrammatic [22–24] and nondiagrammatic [25–27] expansions within the nonequilibrium Green's function (NEGF) formalism [28–33]. NEGF gives access to all time-dependent one-body observables, e.g., particle density, current density, local moments, etc., as well as to the (non)equilibrium spectral functions, and features a power-law scaling with the size. The main drawback of the NEGF is numerical rather than formal; the computational effort required to evolve the system by solving the Kadanoff-Baym equations (KBEs) [28,29]—a *cubic* scaling with the propagation time—limits the simulations to small systems and short times.

In purely electronic systems, the NEGF time scaling can be reduced from cubic to *quadratic* using the so-called generalized Kadanoff-Baym ansatz (GKBA) [34], a controlled approximation which has recently fostered time-dependent studies in inhomogeneous systems, from models, [35–38] to atoms [39] and organic molecules [40–42]. An even lower scaling has been achieved this year, by mapping the GKBA (with mean-field propagators) integro-differential equations onto a coupled system of

ordinary differential equations (ODEs). This ODE scheme scales *linearly* in time [43,44], thus making the NEGF a competitor to the fastest quantum method currently available, i.e., time-dependent DFT [45]. Because of a lack of an EB GKBA, however, this fast pace of progress is confined to purely electronic systems.

This work reports on a threefold advance of the NEGF approach to interacting EB systems. First, we derive an EB GKBA, thereby reducing the computational effort for NEGF EB time-propagations from cubic to quadratic. Second, we rewrite the EB GKBA integro-differential equations as a system of ODEs, achieving *time-linear* scaling for EB systems. Third, we show that the EB GKBA scheme is conserving, i.e., the scheme fulfills all fundamental conservation laws. These ingredients enable us to study e-ph dynamics in an optically excited narrow band-gap insulator and to shed light on the relaxation and nonthermal behavior of acoustic phonons.

The electron-boson Hamiltonian.—We consider an EB system with Hamiltonian $\hat{H}(t)$ given by

$$\hat{H}(t) = \hat{H}_{\mathrm{el}}(t) + \hat{H}_{\mathrm{bos}} + \hat{H}_{\text{el-bos}}(t), \tag{1}$$

a sum of the electronic Hamiltonian $\hat{H}_{\mathrm{el}}(t)$, the bosonic one $\hat{H}_{\mathrm{bos}}$, and the EB interaction $\hat{H}_{\text{el-bos}}(t)$. We do not specify $\hat{H}_{\mathrm{el}}(t)$, which can be any Hermitian combination of field operators $\hat{c}_q$ ($\hat{c}_q^\dagger$) annihilating (creating) an electron with quantum number q. We write the free bosonic part using the displacement $\hat{\phi}_{\mu,1} \equiv (\hat{a}_\mu^\dagger + \hat{a}_\mu)/\sqrt{2}$ and the momentum $\hat{\phi}_{\mu,2} \equiv i(\hat{a}_\mu^\dagger - \hat{a}_\mu)/\sqrt{2}$, where $\hat{a}_\mu$ ($\hat{a}_\mu^\dagger$) annihilates (creates) a boson in mode μ. Introducing the composite index $\bar{\mu} = (\mu, \xi_\mu)$ with $\xi_\mu = 1, 2$, we have

$$\hat{H}_{\mathrm{bos}} = \sum_{\bar{\mu}\bar{\nu}} \Omega_{\bar{\mu}\bar{\nu}} \hat{\phi}_{\bar{\mu}} \hat{\phi}_{\bar{\nu}}, \tag{2}$$

where $[\hat{\phi}_{\bar{\mu}}, \hat{\phi}_{\bar{\nu}}] = \alpha_{\bar{\mu}\bar{\nu}}$ and $\alpha_{\bar{\mu}\bar{\nu}} = \delta_{\mu\nu}\left(\begin{smallmatrix} 0 & i \\ -i & 0 \end{smallmatrix}\right)_{\xi_\mu\xi_\nu}$. For the EB interaction we consider

$$\hat{H}_{\text{el-bos}}(t) = \sum_{\bar{\mu}pq} \lambda^{\bar{\mu}}_{pq}(t) \hat{c}_p^\dagger \hat{c}_q \hat{\phi}_{\bar{\mu}}, \tag{3}$$

with the EB coupling strength $\lambda^{\bar{\mu}}_{pq}$. The formalism, however, is not limited to linear coupling in the bosonic modes [46].

The electron-boson KBE.—In the NEGF formalism the fundamental unknowns are the electronic lesser and greater $G^{\lessgtr}$ single-particle Green's function (GF) and the bosonic counterparts, $D^{\lessgtr}$. They satisfy the KBE, a system of nonlinear integro-differential equations which for the electronic part read (in matrix form)

$$\begin{aligned} [i\vec{\partial}_t - h(t)]G^{\lessgtr}(t,t') &= [\Sigma^{\lessgtr} \cdot G^A + \Sigma^R \cdot G^{\lessgtr}](t,t'), \\ G^{\lessgtr}(t,t')[-i\overleftarrow{\partial}_{t'} - h(t')] &= [G^{\lessgtr} \cdot \Sigma^A + G^R \cdot \Sigma^{\lessgtr}](t,t'), \end{aligned} \tag{4}$$

where $[A \cdot B](t,t') \equiv \int d\bar{t} A(t,\bar{t}) B(\bar{t},t')$, is a real-time convolution and $X^{R/A}(t,t') = \pm\theta[\pm(t-t')][X^>(t,t') - X^<(t,t')]$ is the retarded and advanced function. The quantity Σ is the correlation part of the self-energy, whereas the time-local mean-field part is incorporated in the single-particle Hamiltonian $h(t) = h_{\mathrm{HF}}(t) + h_{\mathrm{bos}}(t)$, where $h_{\mathrm{HF}}(t)$ is the Hartree-Fock Hamiltonian and $h_{\mathrm{bos},pq}(t) = \sum_{\bar{\mu}} \lambda^{\bar{\mu}}_{pq}(t)\phi_{\bar{\mu}}(t)$ is the bosonic potential. The expectation value $\phi_{\bar{\mu}}(t) = \langle \hat{\phi}_{H,\bar{\mu}}(t) \rangle$ (H denotes the Heisenberg picture) fulfills in matrix form

$$\left[i\boldsymbol{\alpha}\frac{d}{dt} - \bar{\boldsymbol{\Omega}} \right] \boldsymbol{\phi}(t) = \sum_{pq} \boldsymbol{\lambda}_{pq}(t) \rho_{qp}(t). \tag{5}$$

In Eq. (5) $\bar{\boldsymbol{\Omega}} \equiv \boldsymbol{\Omega} + \boldsymbol{\Omega}^{\boldsymbol{T}}$ and $\rho(t) \equiv \rho^<(t) = -iG^<(t,t)$ is the electronic single-particle density matrix.

The bosonic GFs are defined using the fluctuation operators $\Delta\hat{\phi}_{H,\bar{\mu}}(t) = \hat{\phi}_{H,\bar{\mu}}(t) - \phi_{\bar{\mu}}(t)$:

$$D^<_{\bar{\mu}\bar{\nu}}(t,t') = -i\langle \Delta\hat{\phi}_{H,\bar{\nu}}(t') \Delta\hat{\phi}_{H,\bar{\mu}}(t) \rangle, \tag{6}$$

and $D^>_{\bar{\mu}\bar{\nu}}(t,t') = D^<_{\bar{\nu}\bar{\mu}}(t',t)$. The expectation value of $\Delta\hat{\phi}_{H,\bar{\mu}}(t)$ is identically zero by construction, a property which simplifies the bosonic KBE [22,47]:

$$\begin{aligned} [i\vec{\partial}_t - \boldsymbol{\alpha}\bar{\boldsymbol{\Omega}}]\boldsymbol{D}^{\lessgtr}(t,t') &= \boldsymbol{\alpha}[\boldsymbol{\Pi}^{\lessgtr} \cdot \boldsymbol{D}^A + \boldsymbol{\Pi}^R \cdot \boldsymbol{D}^{\lessgtr}](t,t'), \\ \boldsymbol{D}^{\lessgtr}(t,t')[-i\overleftarrow{\partial}_{t'} - \bar{\boldsymbol{\Omega}}\boldsymbol{\alpha}] &= [\boldsymbol{D}^{\lessgtr} \cdot \boldsymbol{\Pi}^A + \boldsymbol{D}^R \cdot \boldsymbol{\Pi}^{\lessgtr}](t,t')\boldsymbol{\alpha}, \end{aligned} \tag{7}$$

where $\boldsymbol{\Pi}$ is the bosonic self-energy. In the ϕ-field notation, the bosonic KBEs are first-order in time. The numerical solution of the coupled Eqs. (4) and (7) is demanding (cubic scaling with the number of time steps) and so far achieved only in small model systems [22,24,47,48]. In this work, we consider the *GD* approximation shown diagrammatically in Fig. 1, as

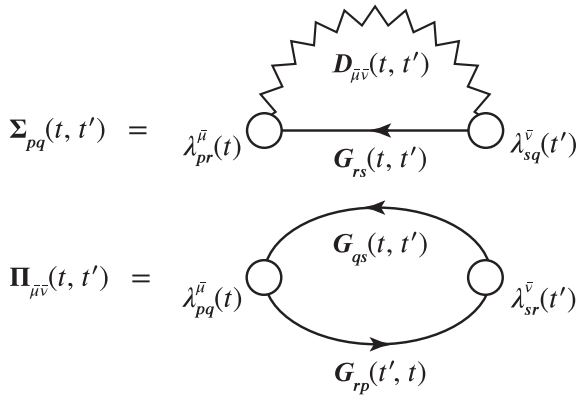

FIG. 1. The *GD* approximation for the electronic (upper panel) and random phase approximation for the bosonic (lower panel) self-energies.

well as the *Gd* ($\Pi = 0$) and mean-field ($\Sigma = \mathbf{\Pi} = 0$, also known as semi-classical Ehrenfest) approximation.

The electron-boson GKBA.—The KBE can be used to generate an equation of motion (EOM) for the electronic density matrix $\rho(t)$ and its bosonic counterpart $\boldsymbol{\rho}_b(t) \equiv \boldsymbol{\rho}_b^<(t) = i\boldsymbol{D}^<(t,t)$. As $\rho(t)$ and $\boldsymbol{\rho}_b(t)$ are single-time functions, their calculation scales quadratically with the number of time steps. Subtracting the two equations in Eqs. (4) and (7) and then letting $t' \to t$ yields

$$\begin{aligned} \partial_t \rho(t) + i[h(t), \rho(t)] &= -[I(t) + I^\dagger(t)], \\ \partial_t \boldsymbol{\rho}_b(t) + i[\boldsymbol{\alpha}\bar{\boldsymbol{\Omega}}\boldsymbol{\rho}_b(t) - \boldsymbol{\rho}_b(t)\bar{\boldsymbol{\Omega}}\boldsymbol{\alpha}] &= \boldsymbol{I}_b(t) + \boldsymbol{I}_b^T(t), \end{aligned} \tag{8}$$

with the electronic and bosonic collision integrals defined as

$$\begin{aligned} I(t) &= \int_0^t d\bar{t}[\Sigma^>(t,\bar{t})G^<(\bar{t},t) - \Sigma^<(t,\bar{t})G^>(\bar{t},t)], \\ \boldsymbol{I}_b(t) &= \boldsymbol{\alpha}\int_0^t d\bar{t}[\mathbf{\Pi}^>(t,\bar{t})\boldsymbol{D}^<(\bar{t},t) - \mathbf{\Pi}^<(t,\bar{t})\boldsymbol{D}^>(\bar{t},t)]. \end{aligned} \tag{9}$$

Evaluation of the collision integrals requires the time-off-diagonal lesser and greater GFs; hence Eq. (8) is not a closed system of equations for the density matrices. A partial rescue is provided by the electronic GKBA [34], i.e., $G^{\lessgtr}(t,t') = \mp[G^R(t,t')\rho^{\lessgtr}(t') - \rho^{\lessgtr}(t)G^A(t,t')]$, where $\rho^>(t) \equiv \hat{\mathbb{1}} - \rho(t)$. Taking $G^R(t,t') = -i\theta(t-t')\mathcal{T}\{\exp(-i\int_{t'}^t h(\bar{t})d\bar{t})\}$, and $G^A(t,t') = [G^R(t',t)]^\dagger$ at the mean-field level, the lesser and greater electronic GF's become functionals of $\rho^<(t)$. However, to close Eq. (9), a GKBA-like form of the lesser and greater bosonic GF is needed.

The form of the electronic GKBA is motivated by the fulfillment of the mean-field KBE, but is augmented with a correlated density matrix. Using the same argument we have derived the *bosonic* GKBA [49]

$$\boldsymbol{D}^{\lessgtr}(t,t') = \boldsymbol{D}^R(t,t')\boldsymbol{\alpha}\boldsymbol{\rho}_b^{\lessgtr}(t') - \boldsymbol{\rho}_b^{\lessgtr}(t)\boldsymbol{\alpha}\boldsymbol{D}^A(t,t'), \tag{10}$$

where $\boldsymbol{\rho}_b^>(t) = \boldsymbol{\alpha} + \boldsymbol{\rho}_b(t)$. Taking $\boldsymbol{D}^{R/A}(t,t') = \mp\, i\boldsymbol{\alpha}\theta[\pm(t-t')]e^{-i\bar{\boldsymbol{\Omega}}\boldsymbol{\alpha}(t-t')}$ at the mean-field level (which coincides with the noninteracting case [22]) the lesser and greater bosonic GFs become functionals of $\boldsymbol{\rho}_b^<(t)$. The bosonic GKBA in Eq. (10) applies even if $\bar{\boldsymbol{\Omega}}$ depends explicitly on time (e. g., phonon driving [55]) [49]. The EB GKBA allows for closing the system in Eq. (8) as both collision integrals I and $\boldsymbol{I}_b$ become functionals of ρ and $\boldsymbol{\rho}_b$. Together with the equation for $\boldsymbol{\phi}$, Eq. (5), the dynamics of any EB system can be simulated.

Conservation laws.—The EB GKBA scheme is conserving, i.e., all fundamental conservation laws are fulfilled provided that the underlying diagrammatic approximation to $\Sigma = \Sigma[G, \boldsymbol{D}]$ and $\mathbf{\Pi} = \mathbf{\Pi}[G, \boldsymbol{D}]$ stems from the functional derivatives of the Baym functional $\Phi[G, \boldsymbol{D}]$ [56] (for the EB case, see, for example, [57,58]). Although Baym's original derivation pertains to self-consistent solutions of the KBE, the whole proof goes through if the rhs's of Eqs. (4) and (7) are evaluated at GF's G' and $\boldsymbol{D}'$ (and hence at Φ-derivable self-energies $\Sigma' = \Sigma[G', \boldsymbol{D}']$ and $\mathbf{\Pi}' = \mathbf{\Pi}[G', \boldsymbol{D}']$) different from the GF's G and $\boldsymbol{D}$ appearing in the lhs. In the Supplemental Material [49] we show that conservation laws are recovered up to terms proportional to the change of $\Phi[G', \boldsymbol{D}']$, as G' and $\boldsymbol{D}'$ are changed according to the transformation having the conserved quantity as generator. Since Φ is invariant under these special transformations the aforementioned terms vanish. In the context of particle conservation this fact was pointed out in Ref. [59] for G' the one-shot GF of an electronic system. The argument is, however, more general and holds for all conservation laws, including energy conservation, as well as EB systems, thereby enlarging enormously the class of conserving approximations.

As the *GD* self-energy is Φ derivable and the GKBA approximation for G and $\boldsymbol{D}$ is one out of the infinitely many choices for G' and $\boldsymbol{D}'$, our scheme is fully conserving and, in particular, it correctly balances the energy transfer from electrons to bosons and viceversa. The *Gd* approximation instead is not Φ derivable, bosons do not feel any feedback from the electrons, and energy conservation is jeopardized.

Linear-time scaling of the electron-boson GKBA.—The EB GKBA computational cost scales quadratically with the number of time steps, as the domain of integration for $I(t)$ and $\boldsymbol{I}_b(t)$ grows linearly in time. Remarkably, the time scaling can be further reduced from quadratic to linear without affecting the scaling with the system size. Let us write the collision integrals of Eq. (9) in the *GD* approximation as

$$\begin{aligned} I_{pl}(t) &= i\sum_{\bar{\mu}r} \lambda_{pr}^{\bar{\mu}}(t)\mathcal{G}_{rl}^{\bar{\mu}}(t), \\ \boldsymbol{I}_b(t) &= -i\sum_{rl}[\boldsymbol{\alpha}\boldsymbol{\lambda}_{rl}(t)] \otimes \boldsymbol{\mathcal{G}}_{lr}(t), \end{aligned} \tag{11}$$

where we introduced the tensor product $(\boldsymbol{v} \otimes \boldsymbol{w})_{\bar{\mu}\bar{\nu}} = v_{\bar{\mu}}w_{\bar{\nu}}$ and the one-time vector $\boldsymbol{\mathcal{G}}_{rl} = \boldsymbol{\mathcal{G}}_{rl}^> - \boldsymbol{\mathcal{G}}_{rl}^<$ with

$$\boldsymbol{\mathcal{G}}_{rl}^{\lessgtr}(t) = \sum_{sq}\int_0^t d\bar{t}\boldsymbol{D}^{\lessgtr}(t,\bar{t})G_{rs}^{\lessgtr}(t,\bar{t})\boldsymbol{\lambda}_{sq}(\bar{t})G_{ql}^{\gtrless}(\bar{t},t). \tag{12}$$

Differentiating Eq. (12) with respect to time yields

$$\begin{aligned} i\frac{d}{dt}\boldsymbol{\mathcal{G}}_{rl}(t) = \boldsymbol{\Psi}_{rl}(t) &+ \boldsymbol{\alpha}\bar{\boldsymbol{\Omega}}\boldsymbol{\mathcal{G}}_{rl}(t) \\ &+ \sum_k [h_{rk}(t)\boldsymbol{\mathcal{G}}_{kl}(t) - \boldsymbol{\mathcal{G}}_{rk}(t)h_{kl}(t)], \end{aligned} \tag{13}$$

with $\boldsymbol{\mathcal{G}}_{rl}(t=0) = 0$, $\boldsymbol{\Psi}_{rl}(t) = \boldsymbol{\Psi}_{rl}^>(t) - \boldsymbol{\Psi}_{rl}^<(t)$, and

$$\mathbf{\Psi}^{\lessgtr}_{rl}(t) = \boldsymbol{\rho}^{\lessgtr}_{b}(t)\sum_{sq}\rho^{\lessgtr}_{rs}(t)\boldsymbol{\lambda}_{sq}(t)\rho^{\gtrless}_{ql}(t). \tag{14}$$

In obtaining Eq. (13) we used the Leibnitz rule of differentiation, $d/dt(\int_0^t d\bar{t} f(t,\bar{t})) = f(t,t) + \int_0^t d\bar{t}(\partial/\partial t) f(t,\bar{t})$, and the fact that the GKBA GFs satisfy the mean-field KBE, i.e., $i(\partial/\partial t)G^{\lessgtr}(t,t') = h(t)G^{\lessgtr}(t,t')$ and $i(\partial/\partial t)\boldsymbol{D}^{\lessgtr}(t,t') = \boldsymbol{\alpha}\bar{\boldsymbol{\Omega}}\boldsymbol{D}^{\lessgtr}(t,t')$. The equations for ρ, $\boldsymbol{\rho}_b$, Eq. (8), and $\boldsymbol{\mathcal{G}}$, Eq. (13), form a closed system of first-order ODEs which is *equivalent* to the original EB GKBA integro-differential equations. Since no integration over time is needed, the EB ODE scheme scales linearly in time.

Numerical algorithms.—We have numerically checked that the integro-differential and ODE formulations of the EB GKBA yield the same results, up to numerical accuracy. We implemented the former scheme in the CHEERS [60] code. The algorithm for the bosonic case follows the electronic algorithm closely, with the difference that the time propagation is nonunitary as $\boldsymbol{\alpha}$ and $\bar{\boldsymbol{\Omega}}$ do not commute. However, by defining the Hermitian matrices $\mathbf{h}_b = (1/2)(\boldsymbol{\alpha}\bar{\boldsymbol{\Omega}} + \bar{\boldsymbol{\Omega}}\boldsymbol{\alpha})$ and $\boldsymbol{\Gamma} = i/2(\boldsymbol{\alpha}\bar{\boldsymbol{\Omega}} - \bar{\boldsymbol{\Omega}}\boldsymbol{\alpha})$, inserting them into the bosonic EOM, and absorbing $\boldsymbol{\Gamma}$ into the collision integral, the bosonic equation gets the same structure as the electronic one and can be solved using the same algorithm. The linear-time propagation is done using the fourth-order Runge-Kutta solver. In the Supplemental Material [49], we provide numerical evidence of the performance and accuracy of the method in the paradigmatic Holstein model, a hallmark of strongly interacting EB systems. The EB GKBA is benchmarked against exact results as well as the full numerical solution of the EB Kadanoff-Baym equations, finding a satisfactory agreement even in the strong-coupling regime. The scaling with the system size is determined by two parameters: the dimension of the electronic basis, N_e, and the number of bosonic modes, N_b. We emphasize that the method does not scale with the number of electrons or bosons. In particular, the scaling is $\mathcal{O}(N_e^3 \times N_b)$ and $\mathcal{O}(N_e^2 \times N_b^2)$ for computing electronic I and bosonic $\boldsymbol{I}_b$ collision integrals, respectively.

Two band model.—To demonstrate the capabilities of our method we turn to periodic systems, specifically a model of a narrow band-gap insulator consisting of one valence v and one conduction c band [61]. Due to system's translational invariance the momentum representation is appropriate:

$$\hat{H}_{\rm el} = \sum_{\alpha,k}\varepsilon_{\alpha k}\hat{c}^{\dagger}_{\alpha k}\hat{c}_{\alpha k} + \frac{1}{N_k}\sum_{q,k,k'}U^{cv}_{q}\hat{c}^{\dagger}_{ck+q}\hat{c}^{\dagger}_{vk'-q}\hat{c}_{vk'}\hat{c}_{ck}. \tag{15}$$

Here U^{cv}_q is the Fourier transform of the interband soft Coulomb interaction $U^{cv}_{ij} = U/\sqrt{|i-j|^2+1}$ and N_k is the number of k points. The e-e interaction is treated at the mean-field level. The electron dispersion $\varepsilon_{\alpha k}$ is described by two parameters: the bandwidth W and the band gap ε_g. Henceforth we express all energies in units of ε_g and choose $U = W/2 = 1$ [61,62]. The electronic system is coupled to a single ($\mu = 1$) phononic branch

$$\hat{H}_{\rm bos} = \sum_{q}\omega_{\mu q}\hat{a}^{\dagger}_{\mu q}\hat{a}_{\mu q}, \quad \omega_{\mu q} = \frac{\omega_D}{\pi}|q|; \tag{16}$$

$$\hat{H}_{\text{el-bos}} = \sum_{k,q}\lambda^{\mu}_{cc}(k,q)\hat{c}^{\dagger}_{ck}\hat{c}_{ck}(\hat{a}^{\dagger}_{\mu q} + \hat{a}_{\mu q}). \tag{17}$$

The coupling is momentum independent, $\lambda^{\mu}_{cc}(k,q) = \lambda_{cc}$. We consider *acoustic* phonons with linear dispersion characterized by the Debye frequency ω_D at the edge of the Brillouin zone $q = \pm\pi$ (in units of inverse lattice spacing). Initially the system is in the ground state, hence the conduction band and the phonons are not populated, $n_e(k) = n_{\rm ph}(k) = 0$. We solve the EB GKBA equations using a mesh of $N_k = 1500$ points. In the k-space formulation the scaling with the system size reduces to $\mathcal{O}(N_k^2)$, see Supplemental Material [49].

In Fig. 2 we present the e-ph dynamics triggered by a laser pulse of frequency $\omega_P = 1.4$. Because $\omega_P > \varepsilon_g$, the c band is populated at nonzero momentum $\pm k_0$ [see the two domes at $t \simeq 0$ in panel (a)]. With electrons in the c band, the e-ph scattering becomes relevant, leading to the creation of phonons, the subsequent redistribution of $n_e(k)$ and $n_{\rm ph}(k)$ occupations and, eventually, to the thermalization of the electrons and low-momentum phonons as well as to the generation and reabsorption of nonthermal phonons [63] around the $\pm k_0$ hot spots. For a typical value of the gap $\varepsilon_g = 1.1$ eV the frequency ω_P corresponds to the 800 nm wavelength of a Ti-sapphire laser. The kinetic energy of the conduction electrons immediately after the pulse is then 0.22 eV yielding for the inverse temperature $\beta = 2.9$ eV^{-1} [64] or approximately $T_e = 4000$ K. At the end of propagation electrons and low-momentum phonons are thermalized, see insets (c) and (d) in Fig. 2, with $\beta \approx 80$, corresponding in our example to $T_e \approx T_{\rm ph} = 160$ K. Signatures of the initially hot phonon distribution do instead persist for much longer times, as can be seen from the side bands at approximately $\pm k_0$. The intermediate stages of the dynamics are more complex, they are characterized by at least two timescales (associated with ω_D and λ^2_{cc}/ω_D) describing the rapid creation of the nonequilibrium phonons and their slow thermalization.

This wealth of phenomena cannot be observed in simpler approaches, such as those based on the two-temperature model [65], semiclassical Boltzmann transport equation [66], or even in NEGF theories with frozen phonons [67–69]. The coupled e-ph dynamics can be studied using the nonequilibrium dynamical mean field theory (DMFT) [70]. However, in this scheme nonlocal correlations are difficult to incorporate [71]. Furthermore, DMFT applications have been so far limited to the Hubbard-Holstein model [72–74] with optical phonons, which simplifies the

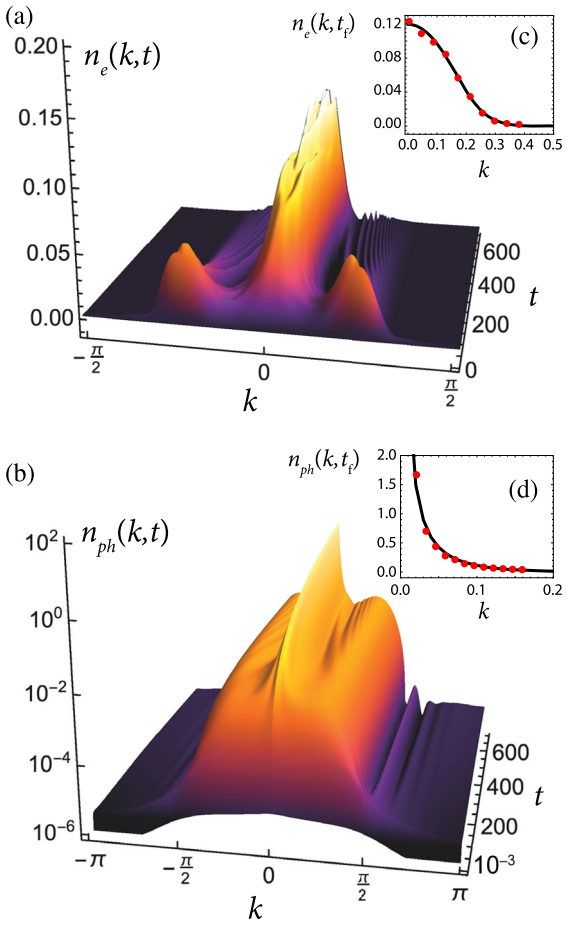

FIG. 2. Relaxation of conduction electrons (a) and acoustic phonons (b) in a two-band model excited with a laser pulse of optical frequency $\omega_P = 1.4$, Rabi frequency $\Omega_P = 0.06$, and pulse duration $T_P = 20$ (energies and times in units of ε_g and ε_g^{-1}, respectively). Electrons are coupled to a branch of acoustic phonons with $\omega_D = 0.8$ and coupling strength $\lambda_{cc} = 0.05$. Insets (c) and (d) depict e and ph populations at the end of the propagation. They can be well fitted with the Fermi-Dirac and the Bose-Einstein distributions at inverse temperature $\beta = 80$.

momentum treatment. Here we demonstrate that it is possible to consider realistic e and ph dispersions and do the propagation linearly in time. Applications to light enhanced superconductivity [5,8,55], formation and melting of the excitonic orders [75], ultrafast band gap control [76], and many other emerging light-induced phenomena [77] are envisaged.

Conclusions.—We have derived an EB GKBA approximation for bosonic propagators and put forward a NEGF scheme to simulate the correlated dynamics of EB systems. The formal advantages of the methods are (i) approximations can be systematically improved by a proper selection of Feynman diagrams and (ii) all fundamental conservation laws are fullfilled provided that the self-energy diagrams are Φ derivable. The energy conservation makes the EB GKBA suitable for studying a plethora of situations where electrons and, for example, phonons can exchange energy; our example being carrier relaxation in a pumped insulator system with acoustic phonons. The computational effort of solving the EB GKBA equations in the ***GD*** approximation scales linearly in time; they can also be implemented in more advanced diagrammatic approximations using the same strategies outlined in Ref. [44]. The inclusion of e-e interactions in the linear-scaling scheme, as discussed in Refs. [43,44], is straightforward. We therefore believe that our proposed method provides an efficient and accurate alternative to the existing computational tools for models as well as first-principles simulations of interacting electrons and bosons out of equilibrium.

D. K. would like to thank the Academy of Finland for funding under Project No. 308697. R. v. L. would like to thank the Academy of Finland for support under Grant No. 317139. G. S., E. P., and Y. P. acknowledge the financial support from MIUR PRIN (Grant No. 20173B72NB), from INFN through the TIME2QUEST project, and from Tor Vergata University through the Beyond Borders Project ULEXIEX.

[1] M. Ruggenthaler, N. Tancogne-Dejean, J. Flick, H. Appel, and A. Rubio, From a quantum-electrodynamical light–matter description to novel spectroscopies, Nat. Rev. Chem. **2**, 0118 (2018).

[2] R. Huber, F. Tauser, A. Brodschelm, M. Bichler, G. Abstreiter, and A. Leitenstorfer, How many-particle interactions develop after ultrafast excitation of an electron-hole plasma, Nature (London) **414**, 286 (2001).

[3] R. Huber, C. Kübler, S. Tübel, A. Leitenstorfer, Q. T. Vu, H. Haug, F. Köhler, and M.-C. Amann, Femtosecond Formation of Coupled Phonon-Plasmon Modes in InP: Ultrabroadband THz Experiment and Quantum Kinetic Theory, Phys. Rev. Lett. **94**, 027401 (2005).

[4] E. Orgiu, J. George, J. A. Hutchison, E. Devaux, J. F. Dayen, B. Doudin, F. Stellacci, C. Genet, J. Schachenmayer, C. Genes, G. Pupillo, P. Samorì, and T. W. Ebbesen, Conductivity in organic semiconductors hybridized with the vacuum field, Nat. Mater. **14**, 1123 (2015).

[5] R. Mankowsky, A. Subedi, M. Först, S. O. Mariager, M. Chollet, H. T. Lemke, J. S. Robinson, J. M. Glownia, M. P. Minitti, A. Frano, M. Fechner, N. A. Spaldin, T. Loew, B. Keimer, A. Georges, and A. Cavalleri, Nonlinear lattice dynamics as a basis for enhanced superconductivity in $YBa_2Cu_3O_{6.5}$, Nature (London) **516**, 71 (2014).

[6] M. Mitrano, A. Cantaluppi, D. Nicoletti, S. Kaiser, A. Perucchi, S. Lupi, P. Di Pietro, D. Pontiroli, M. Riccò, S. R. Clark, D. Jaksch, and A. Cavalleri, Possible light-induced superconductivity in K_3C_{60} at high temperature, Nature (London) **530**, 461 (2016).

[7] M. A. Sentef, A. F. Kemper, A. Georges, and C. Kollath, Theory of light-enhanced phonon-mediated superconductivity, Phys. Rev. B **93**, 144506 (2016).

[8] M. Babadi, M. Knap, I. Martin, G. Refael, and E. Demler, Theory of parametrically amplified electron-phonon superconductivity, Phys. Rev. B **96**, 014512 (2017).

[9] V. Drewello, J. Schmalhorst, A. Thomas, and G. Reiss, Evidence for strong magnon contribution to the TMR temperature dependence in MgO based tunnel junctions, Phys. Rev. B **77**, 014440 (2008).

[10] F. Mahfouzi and B. K. Nikolić, Signatures of electron-magnon interaction in charge and spin currents through magnetic tunnel junctions: A nonequilibrium many-body perturbation theory approach, Phys. Rev. B **90**, 045115 (2014).

[11] N. R. Abdullah, C.-S. Tang, A. Manolescu, and V. Gudmundsson, Effects of photon field on heat transport through a quantum wire attached to leads, Phys. Lett. A **382**, 199 (2018).

[12] H. Walther, B. T. H. Varcoe, B.-G. Englert, and T. Becker, Cavity quantum electrodynamics, Rep. Prog. Phys. **69**, 1325 (2006).

[13] J. A. Hutchison, T. Schwartz, C. Genet, E. Devaux, and T. W. Ebbesen, Modifying chemical landscapes by coupling to vacuum fields, Angew. Chemie—Int. Ed. **51**, 1592 (2012).

[14] B. F. E. Curchod and T. J. Martínez, Ab Initio nonadiabatic quantum molecular dynamics, Chem. Rev. **118**, 3305 (2018).

[15] B. Kloss, D. R. Reichman, and R. Tempelaar, Multiset Matrix Product State Calculations Reveal Mobile Franck-Condon Excitations Under Strong Holstein-Type Coupling, Phys. Rev. Lett. **123**, 126601 (2019).

[16] L. Pollet, Recent developments in quantum Monte Carlo simulations with applications for cold gases, Rep. Prog. Phys. **75**, 094501 (2012).

[17] G. Cohen, E. Gull, D. R. Reichman, and A. J. Millis, Taming the Dynamical Sign Problem in Real-Time Evolution of Quantum Many-Body Problems, Phys. Rev. Lett. **115**, 266802 (2015).

[18] H. Ma, Z. Luo, and Y. Yao, The time-dependent density matrix renormalisation group method, Mol. Phys. **116**, 854 (2018).

[19] M. Ruggenthaler, J. Flick, C. Pellegrini, H. Appel, I. V. Tokatly, and A. Rubio, Quantum-electrodynamical density-functional theory: Bridging quantum optics and electronic-structure theory, Phys. Rev. A **90**, 012508 (2014).

[20] C. Schäfer, M. Ruggenthaler, and A. Rubio, Ab initio nonrelativistic quantum electrodynamics: Bridging quantum chemistry and quantum optics from weak to strong coupling, Phys. Rev. A **98**, 043801 (2018).

[21] R. Jestädt, M. Ruggenthaler, M. J. T. Oliveira, A. Rubio, and H. Appel, Light matter interactions within the ehrenfest-maxwell-pauli-kohn-sham framework: Fundamentals, implementation, and nano-optical applications, Adv. Phys. **68**, 225 (2019).

[22] N. Säkkinen, Y. Peng, H. Appel, and R. van Leeuwen, Many-body Green's function theory for electron-phonon interactions: The Kadanoff-Baym approach to spectral properties of the Holstein dimer, J. Chem. Phys. **143**, 234102 (2015).

[23] P. M. M. C. de Melo and A. Marini, Unified theory of quantized electrons, phonons, and photons out of equilibrium: A simplified ab initio approach based on the generalized Baym-Kadanoff ansatz, Phys. Rev. B **93**, 155102 (2016).

[24] M. Schüler, J. Berakdar, and Y. Pavlyukh, Time-dependent many-body treatment of electron-boson dynamics: Application to plasmon-accompanied photoemission, Phys. Rev. B **93**, 054303 (2016).

[25] P. Werner and M. Eckstein, Phonon-enhanced relaxation and excitation in the Holstein-Hubbard model, Phys. Rev. B **88**, 165108 (2013).

[26] Y. Murakami, P. Werner, N. Tsuji, and H. Aoki, Multiple amplitude modes in strongly coupled phonon-mediated superconductors, Phys. Rev. B **93**, 094509 (2016).

[27] D. Hügel, P. Werner, L. Pollet, and H. U. R. Strand, Bosonic self-energy functional theory, Phys. Rev. B **94**, 195119 (2016).

[28] L. V. Keldysh, Diagram technique for nonequilibrium processes, Sov. Phys. JETP **20**, 1018 (1965), http://www.jetp.ac.ru/cgi-bin/e/index/e/20/4/p1018?a=list.

[29] L. P. Kadanoff and G. Baym, *Quantum Statistical Mechanics* (Benjamin, New York, 1962).

[30] P. Danielewicz, Quantum theory of nonequilibrium processes, Ann. Phys. (N.Y.) **152**, 239 (1984).

[31] H. Haug and A. P. Jauho, *Quantum Kinetics in Transport and Optics of Semiconductors*, Solid-State Sciences Vol. 123 (Springer Berlin Heidelberg, Berlin, Heidelberg, 2008).

[32] G. Stefanucci and R. van Leeuwen, *Nonequilibrium Many-Body Theory Quantum Syst. A Mod. Introd.* (Cambridge University Press, Cambridge, England, 2013).

[33] K. Balzer and M. Bonitz, *Nonequilibrium Green's Functions Approach to Inhomogeneous Systems*, Lecture Notes in Physics Vol. 867 (Springer Berlin Heidelberg, Berlin, Heidelberg, 2013).

[34] P. Lipavský, V. Špička, and B. Velický, Generalized Kadanoff-Baym ansatz for deriving quantum transport equations, Phys. Rev. B **34**, 6933 (1986).

[35] S. Hermanns, N. Schlünzen, and M. Bonitz, Hubbard nanoclusters far from equilibrium, Phys. Rev. B **90**, 125111 (2014).

[36] S. Latini, E. Perfetto, A.-M. Uimonen, R. van Leeuwen, and G. Stefanucci, Charge dynamics in molecular junctions: Nonequilibrium Green's function approach made fast, Phys. Rev. B **89**, 075306 (2014).

[37] N. Schlünzen, J.-P. Joost, F. Heidrich-Meisner, and M. Bonitz, Nonequilibrium dynamics in the one-dimensional fermi-hubbard model: Comparison of the nonequilibrium Green-functions approach and the density matrix renormalization group method, Phys. Rev. B **95**, 165139 (2017).

[38] E. V. Boström, A. Mikkelsen, C. Verdozzi, E. Perfetto, and G. Stefanucci, Charge separation in donor-C_{60} complexes with real-time Green functions: The importance of nonlocal correlations, Nano Lett. **18**, 785 (2018).

[39] E. Perfetto, A.-M. Uimonen, R. van Leeuwen, and G. Stefanucci, First-principles nonequilibrium Green's-function approach to transient photoabsorption: Application to atoms, Phys. Rev. A **92**, 033419 (2015).

[40] E. Perfetto, D. Sangalli, A. Marini, and G. Stefanucci, Ultrafast charge migration in XUV photoexcited phenylalanine: A first-principles study based on real-time nonequilibrium Green's functions, J. Phys. Chem. Lett. **9**, 1353 (2018).

[41] E. Perfetto, D. Sangalli, M. Palummo, A. Marini, and G. Stefanucci, First-principles nonequilibrium Green's function approach to ultrafast charge migration in glycine, J. Chem. Theory Comput. **15**, 4526 (2019).
[42] E. Perfetto, A. Trabattoni, F. Calegari, M. Nisoli, A. Marini, and G. Stefanucci, Ultrafast quantum interference in the charge migration of tryptophan, J. Phys. Chem. Lett. **11**, 891 (2020).
[43] N. Schlünzen, J.-P. Joost, and M. Bonitz, Achieving the Scaling Limit for Nonequilibrium Green Functions Simulations, Phys. Rev. Lett. **124**, 076601 (2020).
[44] J.-P. Joost, N. Schlünzen, and M. Bonitz, G1-G2 scheme: Dramatic acceleration of nonequilibrium Green functions simulations within the Hartree-Fock generalized Kadanoff-Baym ansatz, Phys. Rev. B **101**, 245101 (2020).
[45] C. A. Ullrich, *Time-Dependent Density-Functional Theory* (Oxford University Press, Oxford, 2012).
[46] A. Marini and Y. Pavlyukh, Functional approach to the electronic and bosonic dynamics of many-body systems perturbed with an arbitrary strong electron-boson interaction, Phys. Rev. B **98**, 075105 (2018).
[47] D. Karlsson and R. van Leeuwen, Non-equilibrium Green's functions for coupled fermion-boson systems, in *Handbook of Materials Modeling*, edited by W. Andreoni and S. Yip (Springer International Publishing, Cham, 2018), pp. 1–29.
[48] N. Säkkinen, Y. Peng, H. Appel, and R. van Leeuwen, Many-body Green's function theory for electron-phonon interactions: Ground state properties of the Holstein dimer, J. Chem. Phys. **143**, 234101 (2015).
[49] See Supplemental Material at http://link.aps.org/supplemental/10.1103/PhysRevLett.127.036402 for a derivation of the EB GKBA, a proof of energy conservation, and benchmarks against exact and KBE results, which includes Refs. [50–54].
[50] M. Hopjan and C. Verdozzi, Initial correlated states for the generalized Kadanoff–Baym Ansatz without adiabatic switching-on of interactions in closed systems, Eur. Phys. J. Special Topics **227**, 1939 (2019).
[51] J. T. Devreese and A. S. Alexandrov, Fröhlich polaron and bipolaron: Recent developments, Rep. Prog. Phys. **72**, 066501 (2009).
[52] P. Weinberg and M. Bukov, QuSpin: A Python package for dynamics and exact diagonalisation of quantum many body systems part I: Spin chains, SciPost Phys. **2**, 003 (2017).
[53] P. Weinberg and M. Bukov, QuSpin: A Python package for dynamics and exact diagonalisation of quantum many body systems. Part II: Bosons, fermions and higher spins, SciPost Phys. **7**, 020 (2019).
[54] M. Puig von Friesen, C. Verdozzi, and C.-O. Almbladh, Kadanoff-Baym dynamics of Hubbard clusters: Performance of many-body schemes, correlation-induced damping and multiple steady and quasi-steady states, Phys. Rev. B **82**, 155108 (2010).
[55] M. Först, C. Manzoni, S. Kaiser, Y. Tomioka, Y. Tokura, R. Merlin, and A. Cavalleri, Nonlinear phononics as an ultrafast route to lattice control, Nat. Phys. **7**, 854 (2011).
[56] G. Baym, Self-consistent approximations in many-body systems, Phys. Rev. **127**, 1391 (1962).
[57] N. Säkkinen, Application of time-dependent many-body perturbation theory to excitation spectra of selected finite model systems, Ph.D. thesis, University of Jyväskylä, 2016.
[58] I. V. Tokatly, Conserving approximations in cavity quantum electrodynamics: Implications for density functional theory of electron-photon systems, Phys. Rev. B **98**, 235123 (2018).
[59] H. Mera, M. Lannoo, C. Li, N. Cavassilas, and M. Bescond, Inelastic scattering in nanoscale devices: One-shot current-conserving lowest-order approximation, Phys. Rev. B **86**, 161404(R) (2012).
[60] E. Perfetto and G. Stefanucci, CHEERS: a tool for correlated hole-electron evolution from real-time simulations, J. Phys. Condens. Matter **30**, 465901 (2018).
[61] E. Perfetto and G. Stefanucci, Floquet Topological Phase of Nondriven p-Wave Nonequilibrium Excitonic Insulators, Phys. Rev. Lett. **125**, 106401 (2020).
[62] E. Perfetto, D. Sangalli, A. Marini, and G. Stefanucci, Pump-driven normal-to-excitonic insulator transition: Josephson oscillations and signatures of BEC-BCS crossover in time-resolved ARPES, Phys. Rev. Mater. **3**, 124601 (2019).
[63] Y. Yang, D. P. Ostrowski, R. M. France, K. Zhu, J. van de Lagemaat, J. M. Luther, and M. C. Beard, Observation of a hot-phonon bottleneck in lead-iodide perovskites, Nat. Photonics **10**, 53 (2016).
[64] By assuming parabolic dispersion of the conduction electrons at small-k it follows $E_K = -\zeta_{3/2}/[2^{3/2}\zeta_{1/2}\beta] = 0.63/\beta$.
[65] T. Shin, S. W. Teitelbaum, J. Wolfson, M. Kandyla, and K. A. Nelson, Extended two-temperature model for ultrafast thermal response of band gap materials upon impulsive optical excitation, J. Chem. Phys. **143**, 194705 (2015).
[66] S. Sadasivam, M. K. Y. Chan, and P. Darancet, Theory of Thermal Relaxation of Electrons in Semiconductors, Phys. Rev. Lett. **119**, 136602 (2017).
[67] A. F. Kemper, M. A. Sentef, B. Moritz, J. K. Freericks, and T. P. Devereaux, Direct observation of Higgs mode oscillations in the pump-probe photoemission spectra of electron-phonon mediated superconductors, Phys. Rev. B **92**, 224517 (2015).
[68] D. Sangalli and A. Marini, Ultra-fast carriers relaxation in bulk silicon following photo-excitation with a short and polarized laser pulse, Europhys. Lett. **110**, 47004 (2015).
[69] Y. Murakami, M. Schüler, S. Takayoshi, and P. Werner, Ultrafast nonequilibrium evolution of excitonic modes in semiconductors, Phys. Rev. B **101**, 035203 (2020).
[70] J. K. Freericks, V. M. Turkowski, and V. Zlatić, Nonequilibrium Dynamical Mean-Field Theory, Phys. Rev. Lett. **97**, 266408 (2006).
[71] S. Biermann, F. Aryasetiawan, and A. Georges, First-Principles Approach to the Electronic Structure of Strongly Correlated Systems: Combining the GW Approximation and Dynamical Mean-Field Theory, Phys. Rev. Lett. **90**, 086402 (2003).
[72] Y. Murakami, P. Werner, N. Tsuji, and H. Aoki, Interaction quench in the Holstein model: Thermalization crossover from electron- to phonon-dominated relaxation, Phys. Rev. B **91**, 045128 (2015).
[73] Y. Murakami, N. Tsuji, M. Eckstein, and P. Werner, Nonequilibrium steady states and transient dynamics of conventional superconductors under phonon driving, Phys. Rev. B **96**, 045125 (2017).

[74] Y. Murakami, P. Werner, N. Tsuji, and H. Aoki, Multiple amplitude modes in strongly coupled phonon-mediated superconductors, Phys. Rev. B **93**, 094509 (2016).

[75] S. Hellmann, T. Rohwer, M. Kalläne, K. Hanff, C. Sohrt, A. Stange, A. Carr, M. M. Murnane, H. C. Kapteyn, L. Kipp, M. Bauer, and K. Rossnagel, Time-domain classification of charge-density-wave insulators, Nat. Commun. **3**, 1069 (2012).

[76] S. Mor, M. Herzog, D. Golež, P. Werner, M. Eckstein, N. Katayama, M. Nohara, H. Takagi, T. Mizokawa, C. Monney, and J. Stähler, Ultrafast Electronic Band Gap Control in an Excitonic Insulator, Phys. Rev. Lett. **119**, 086401 (2017).

[77] D. N. Basov, R. D. Averitt, and D. Hsieh, Towards properties on demand in quantum materials, Nat. Mater. **16**, 1077 (2017).